IMA Chromatography of a Cell Extract: Effect of Loading pH on Protein Purification

Anshuman V. Patwardhan and Mohammad M. Ataai
Dept. of Chemical Engineering, and The Center for Biotechnology and Bioengineering, University of Pittsburgh, Pittsburgh, PA 15219

Immobilized metal ion affinity chromatography has shown promise for isolating desired proteins from host cell extracts, based on differential affinities for chelated metal ions. This article focuses on modeling the effect of loading pH on the purity and binding capacity of target proteins, during their separation from the cell extract of Escherichia coli, using immobilized copper affinity chromatography. Early chromatography experiments revealed that cellular proteins of E. coli elute in two separate peaks from an immobilized copper column under a decreasing pH step gradient. Thus, the cell extract is modeled by a mixture of two proteins, tuna heart cytochrome c and chicken egg white lysozyme. Transport and binding parameters of these proteins are evaluated over a wide pH range and used in a mathematical model of multicomponent chromatography. Target proteins are chosen such that they elute at a pH between the elution pH of cytochrome and lysozyme. Simulation results showed that decreasing the loading pH to a value between the elution pH of the weaker copper binding proteins of E. coli and that of the target protein may not only decrease the amount of E. coli proteins bound in the column but lead to a substantially higher binding capacity for the target protein.

Introduction

Immobilized metal ion affinity chromatography (IMAC), introduced by Porath and coworkers (1975), is a powerful tool used in the separation of proteins. The technique consists of passing a mixture of proteins through a column packed with porous beads that are functionalized with metal chelating groups such as imminodiacetic acid (IDA) or nitrilotriacetic acid (NTA). These groups serve as chelating moieties for metals (Cu, Zn, Co, Ni, Fe) that have affinity for the protein of interest. Since the interaction between proteins and metal is pH dependent, elution can be performed by developing a linear, nonlinear, or a stepwise gradient in pH. Low cost of the matrix, ease of regeneration, and the specificity of protein–metal interactions are among the key advantages of IMAC. A wide variety of native proteins, displaying favorable metal binding characteristics, have been purified using immobilized Cu, Ni, Zn, Co, and Fe columns (Porath and Olin, 1983; Anderson et al., 1991; Beitle and Ataai, 1992). Moreover, recombinant DNA technology has allowed the use of IMAC for the purification of many proteins with insignificant metal binding, by their fusion to a metal-binding peptide, as an affinity tail (Hochuli et al., 1988; Vosters et al., 1992; Beitle and Ataai, 1993). A tail consisting of six adjacent histidines (His_6) has frequently been used for the purification of a large number of different proteins (Hochuli et al., 1988; Le Grice and Leitch, 1990; Crowe et al., 1994). Recently, techniques have been developed in our laboratory for the selection of optimum affinity tails that will endow a target protein with the "right amount of" metal affinity and lead to high purification factors in one IMAC step. These developments are based on screening phage displayed random hexapeptide libraries, typically containing more than 10,000,000 different peptides (Goud et al., 1996; Patwardhan et al., 1977 (a, b).

The goal of this article is to establish the optimum pH for the loading of a cell extract containing a target protein of given metal affinity, of its own or imparted to it by its fusion to an affinity tail, that will lead to a higher capacity and resolution of the target protein. In early experiments, we performed the chromatography of the cell extract of the bacterium *Escherichia coli,* the most widely used host cell for the production of recombinant proteins, on an immobilized cop-

Correspondence concerning this article should be addressed to M. M. Ataai.

per (Cu-IDA) column (Patwardhan and Ataai, 1996). The extract was loaded at pH 7.5 and eluted with a decreasing pH step gradient from pH 7.5 to 4, followed by an EDTA wash (EDTA: a strong chelating agent, used to remove metals and tightly bound proteins from the column). Most of the cellular proteins exhibited minimal binding to Cu-IDA and eluted above pH 7, while a majority of the remaining proteins bound strongly and eluted below pH 5 (pH 4.0 and EDTA fractions). Thus, the chromatography behavior of the *E. coli* cell extract, which may contain several thousand different proteins, could approximately be modeled using a mixture of two proteins.

We have selected a mixture of tuna heart cytochrome c and chicken egg white lysozyme to represent the *E. coli* cell extract. Cytochrome and lysozyme elute from Cu-IDA at pH 7 and 5, respectively (Hemdan et al., 1989). The mass-transfer coefficients and the binding parameters (i.e., the equilibrium binding constants with Cu-IDA and the saturation capacity) of these proteins were evaluated over a wide pH range and incorporated into a detailed mathematical model of multicomponent chromatography. Multicomponent chromatography models have proved useful for the theoretical assessment of the chromatography behavior of proteins and other mixtures (Golshan-Shirazi and Guiochon, 1989; Velayudhan et al., 1992; Binous and McCoy, 1992). The model accounts for four components: two proteins (cytochrome and lysozyme), to represent the *E. coli* cell extract, one target protein, and hydrogen ions. The pH dependence of the binding constants of the target protein to Cu-IDA was selected such that it would elute at a pH between the elution pH of cytochrome and lysozyme. Model predictions were experimentally validated for individual proteins as well as for the mixture.

Simulation results demonstrate that loading the mixture at a pH lower than the elution pH of the weaker copper binding proteins of *E. coli* (represented by cytochrome), but above that of the target protein, not only leads to a substantial decrease in the amount of impurities but also to a higher column capacity for the target protein.

Mathematical Model

The mathematical model incorporates the effects of axial dispersion, intraparticle diffusion, film mass transfer, and adsorption–desorption kinetics. The assumptions made are fast kinetics, negligible concentration gradients in the radial direction, and constant mass-transfer parameters, independent of adsorbed concentration.

Model equations

Material balance over a differential height in the column, on the bulk liquid phase, pore liquid phase, and adsorbed phase led to the following system of coupled partial differential equations

$$\frac{\partial C_{b_i}}{\partial t} = D_{b_i}\frac{\partial^2 C_{b_i}}{\partial x^2} - \frac{\upsilon}{\epsilon_b}\frac{\partial C_{b_i}}{\partial x} - \frac{3k_i(1-\epsilon_b)}{\epsilon_b R} \times [C_{b_i} - (C_{p_i, r=R}/k_{\mathrm{prt},i})] \quad (1)$$

$$\frac{\partial C_{p_i}}{\partial t} = \frac{1}{\epsilon_{p_i}}\frac{\partial q_i}{\partial t} - D_{p_i}\left[\frac{1}{r^2}\frac{\partial}{\partial r}\left(r^2\frac{\partial C_{p_i}}{\partial r}\right)\right] \quad (2)$$

$$\frac{\partial q_i}{\partial t} = k_{a_i}C_{p_i}\left(q_{mi} - \sum_{j=1}^{n} q_j\right) - k_{d_i}q_i, \quad (3)$$

where

$$k_{d_i} = \frac{k_{a_i}}{B_i}.$$

For the case of fast kinetics (i.e., large value of k_{a_i} and k_{d_i}) (Gu et al., 1992; Whitley et al., 1994), Eq. 3 reduces to the multicomponent Langmuir isotherm:

$$q_i = \frac{q_{m_i}B_iC_{p_i}}{1 + \sum_{j=1}^{n} B_jC_{p_j}}. \quad (4)$$

Equation 3 becomes thermodynamically inconsistent when the saturation capacities of the individual proteins are different. As suggested by Gu et al. (1991), the problem was eliminated by using "discount factors" to normalize the adsorbed concentrations to the same scale. Using this approach, Eq. 3 becomes:

$$\frac{\partial q_i}{\partial t} = k_{a_i}C_{p_i}\left(q_{mi} - \sum_{j=1}^{n} q_j\delta_{ij}\right) - k_{d_i}q_i, \quad (5)$$

where, $\delta_{ij} = q_{mi}/q_{mj}$.

The adsorption of modulator ions (hydrogen ions in this case) can also be modeled using kinetic equations or nonlinear equilibrium isotherm (Velayudhan and Ladisch, 1995). Hydrogen ions cannot be viewed in IMAC elution as classic modulators. This is because they do not compete with the protein for the affinity ligand, rather their effect is due to the protonation of the binding residue(s) of the protein. Apart from binding to protein residues, hydrogen ions may also weakly bind to various components inside the column, including the stationary phase and the spacer arm. For simplicity purposes, these interactions are approximated in the model by a lumped retention factor $K_{\mathrm{H,lin}}$ of a linear isotherm:

$$q_{\mathrm{H}} = K_{\mathrm{H,lin}}C_{p_{\mathrm{H}}}. \quad (6)$$

The value of $K_{\mathrm{H,lin}}$ is determined by fitting the predicted step in the exit pH, during a decreasing step pH gradient elution, with the measured exit pH.

Initial and boundary conditions

$$t = 0; \quad C_{b_i} = C_{b_i}(0, x) \quad (7)$$

$$C_{p_i} = C_{p_i}(0, r, x)$$

$$q_i = q_i(0, r, x)$$

$$x = 0; \quad \frac{\partial C_{b_i}}{\partial x} = \frac{\upsilon}{D_{P_i}\epsilon_b}[C_{b_i} - C_{f_i}(t)] \tag{8}$$

$C_{f_i}(t) = C_{f_i}$ for adsorption

$C_{f_i}(t) = 0$ for elution

(since elution is accomplished by buffers of different pH values without any protein)

$$x = H, \quad \frac{\partial C_{b_i}}{\partial x} = 0 \tag{9}$$

$$r = 0, \quad \frac{\partial C_{p_i}}{\partial r} = 0 \tag{10}$$

$$r = R, \quad \frac{\partial C_{p_i}}{\partial r} = \frac{k_i}{\epsilon_{p_i} D_{p_i}}[C_{b_i} - (C_{p_i, r=R}/k_{prt})] \tag{11}$$

Numerical solution

The preceding system of partial differential equations was discretized using the method of orthogonal collocation (OC) for the particle phase and the method of orthogonal collocation over fixed finite elements (OCFE) in the axial direction for the column. The resultant system of ordinary differential equations was solved using the subroutine DIVPAG from IMSL (1991). The simulations were performed on a DEC-3000 Model-400 VMS workstation, with two finite elements, five axial collocation points for the column, and four radial collocation points for the particle phase.

Experimental Methods

Chromatography experiments

Highest grade chicken egg white lysozyme (MW: 14,300) and tuna heart cytochrome c (MW: 12,700) were purchased from Sigma Chemicals (St. Louis, MO). All the other chemicals were reagent grade. The experimental setup consisted of a glass column (1 cm ID), a peristaltic pump P-1 (Pharmacia Biotech., Piscataway, NJ), and a fraction collector, FRAC-100 (Pharmacia Biotech., Piscataway, NJ). The column was packed with Chelating Sepharose Fast Flow Gel (Pharmacia Biotech, Piscataway, NJ). The gel was washed and degassed before packing. The height of the packed bed was 2.55 cm. After each run, the column was regenerated for the next run by passing six column volumes of a solution of 50-mM EDTA in 20-mM sodium phosphate buffer (0.5-M NaCl, pH 7.0) to remove copper and the remaining bound proteins (0.5-M NaCl is included in IMAC buffers in order to suppress ionic interactions). The column was then washed with 0.1-M acetate buffer (0.5-M NaCl, pH 4) to remove EDTA. The column was reloaded with copper by passing 50-mM $CuSO_4$ in 0.1-M sodium acetate buffer (0.5-M NaCl, pH 4.0). Finally, six column volumes of the loading buffer of a suitable pH were passed in order to equilibrate the column. The preceding procedure was rigorously followed before each experiment in order to ensure uniform copper loading.

Breakthrough Experiments. Breakthrough experiments were performed to obtain the values of B and q_m for lysozyme. An appropriate amount of lysozyme was dissolved in the equilibration buffer and the pH of the solution was checked. The pH tended to change by small amounts (< 0.1 pH units), especially at high protein concentrations. After adjusting the pH, the solution was applied to the column at a flow rate of 0.4 mL/min until saturation. The exit protein concentration from the column was measured by optical density measurements at a wavelength of 280 nm using an on-line UV detector (Pharmacia LKB Uvicord SII). The output of the UV detector was fed to a chart recorder (Fisher Recordall Series 5000, Fisher Scientific, PA). The pH of the eluted fractions was measured using pH meter 220 from Corning (Corning, NY). No significant difference between the inlet and outlet pH was observed (< 0.05 units).

Zonal Analysis. Zonal analysis experiments were performed to obtain the values of the product of B and q_m for cytochrome at different pH values (Dunn, 1984). A small pulse of cytochrome (containing approximately 10 μg cytochrome), dissolved in the buffer of a suitable pH, was applied to the column and washed with the same buffer at 0.4 mL/min. The outlet concentration was monitored using the UV detector. All peaks were symmetrical in nature, indicating operation in the linear range of the Langmuir isotherm (Arnold et al., 1986).

Chromatography of the E. coli Cell Extract. *E. coli* cells (JM101, American Type Cell Culture No. 33876) were grown at 37°C in a 30 g/L LB broth. The cells were harvested at $OD_{600\ nm}$ of 0.5 by centrifugation at 10,000 rpm for 10 min and resuspended in 5 mL of 20-mM sodium phosphate buffer (0.5-MNaCl, pH 7.3). This step was followed by French pressing at 20,000 psi (138 MPa) to release the intracellular material. The intracellular protein was recovered in the supernatant after centrifuging at 10,000 rpm for 15 min. The supernatant was diluted 100-fold in the 20-mM sodium phosphate buffer (0.5-M NaCl, pH 7.5) and loaded onto the column at 0.4 mL/min. The bound proteins were eluted with a decreasing pH step gradient from pH 7.5 to 4, followed by EDTA treatment. The eluted fractions were analyzed using sodium dodecyl sulfate polyacrylamide gel electrophoresis (SDS-PAGE). The bands (representing different proteins) on the gel (15% polyacrylamide) were visualized using the Bio-Rad silver staining kit (Silver Stain Plus, BioRad, Melville, NY). The gel was also overexposed in order to detect *E. coli* proteins present at very low levels.

Results and Discussion

Figure 1a shows the result of the chromatography of *E. coli* cell extract on a Cu-IDA column. The *E. coli* cell extract was loaded at pH 7.5 and eluted with a decreasing pH step gradient from 7.5 to 4, followed by an EDTA treatment. A majority of cellular proteins eluted in two fractions, one eluting above pH 7.0 and the other eluting below pH 5.0. Figure 1b shows the SDS-PAGE of the proteins eluted at various pH values. This technique allows for very small amounts of proteins to become visible [2 ng protein per band (personal communication with BioRad Laboratories, Melville, NY)]. Despite the high sensitivity of the silver stained gel, a "contaminant-free window" is apparent in the elution profile of *E. coli* proteins. Thus, it is very reasonable to group the *E. coli* proteins into two fractions. One group will represent those proteins that elute above pH 7 (i.e., the flowthrough

fraction and the fractions eluted at pH 7.5 and 7: Figure 1b), and the other group will represent proteins that emerge from the column at pH values below 5.0 (pH 4 and EDTA fractions). These two groups of proteins were represented in our model by tuna heart cytochrome c and chicken egg white lysozyme. Cytochrome and lysozyme elute from Cu-IDA at pH 7 and 5, respectively (Hemdan et al., 1989). The determination of the transport and binding parameters of these two proteins with Cu-IDA is described next.

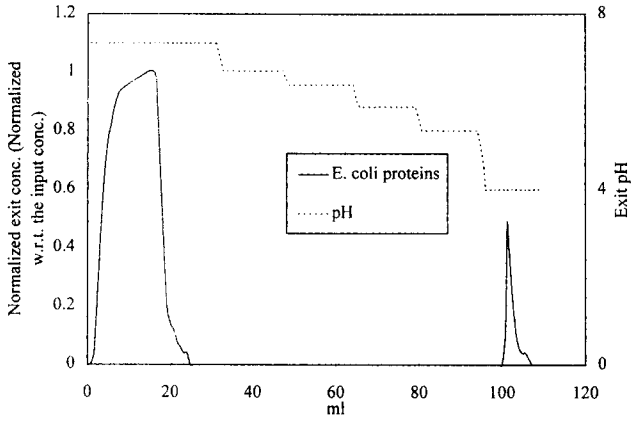

Figure 1(a). Cu-IDA chromatography of the *E. coli* cell extract.

700 μL of *E. coli* cell extract (pH 7.4) dissolved in 55 mL of 20-mM sodium phosphate buffer (0.5 M NaCl, pH 7.5) was loaded onto the column and the bound proteins are eluted with a decreasing pH step gradient (16 ml at each pH). The exit protein concentration is measured by optical density measurements at 280 nM. The arrow represents the end of loading and beginning of elution.

Estimation of model parameters

The transport parameters for proteins and hydrogen ions are estimated using literature correlations. The values of all the parameters, along with the correlations used to estimate them, are listed in Table 1.

The parameters of the Langmuir isotherm, namely, the saturation capacity (q_m) of the matrix and the binding constant (B) between proteins and Cu-IDA were determined for cytochrome and lysozyme over the entire pH range of operation. Breakthrough and zonal analysis experiments were performed to evaluate the binding constant between lysozyme and Cu-IDA and cytochrome and Cu-IDA, respectively.

Lysozyme. The values of B and q_m are available for lysozyme at pH 7.0 (Hutchens et al., 1988). First, these values were used in the model to simulate the breakthrough curve at pH 7. Figure 2 shows the comparison between the experimental breakthrough curve and the simulated one. Clearly, the correspondence between the predicted and the measured breakthrough curves, without any adjustment of the parameters, is impressive. In order to further improve the fit, the saturation capacity was adjusted to a value about 5% lower than the published value (Table 1). The simulation with the adjusted value is shown by a dotted line that essentially overlaps the measured breakthrough curve. This value of q_m was used in further simulations. The values of B at different pH

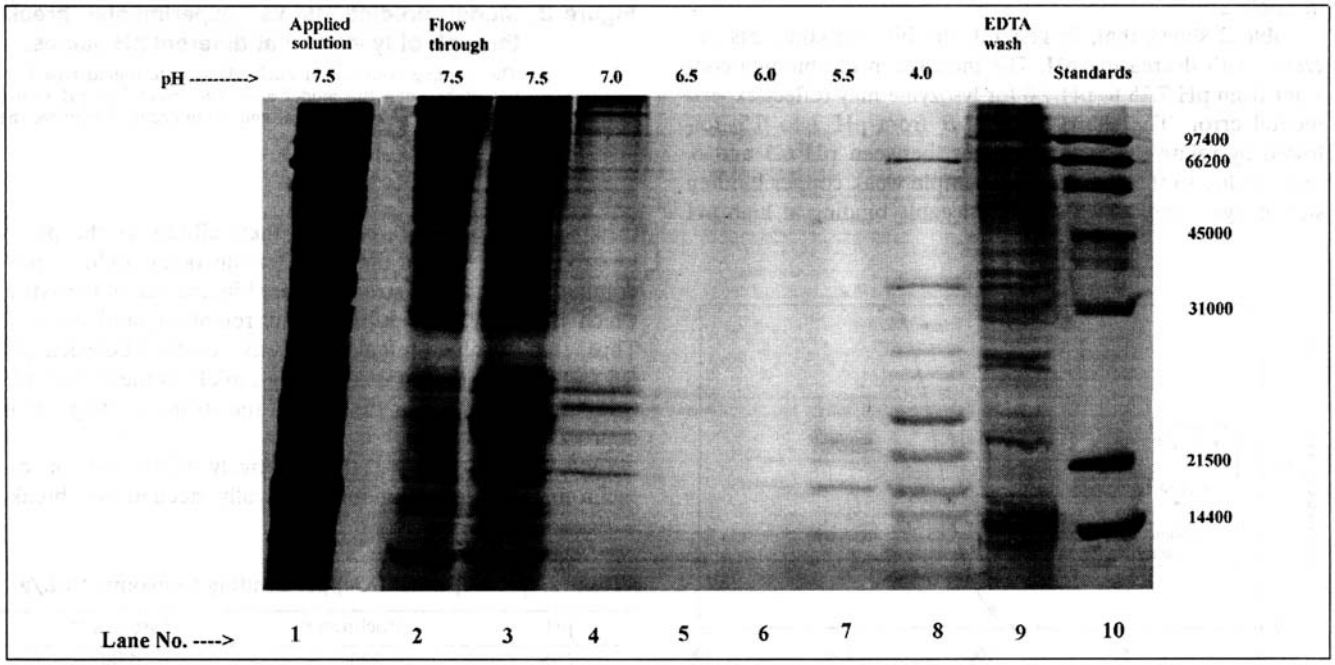

Figure 1(b). SDS-PAGE of the IMAC fractions.

The gel is silver stained and overexposed to show minor contaminants. 200μL of *E. coli* cell extract (pH 7.5) dissolved in 10 mL of 20-mM sodium phosphate buffer (0.5-M NaCl, pH 7.5) served as the input sample (Lane 1). Lane 2 is the unbound proteins eluted during loading. A step gradient of pH (7 column volumes at each pH) was used to elute the bound proteins. Lanes 3 to 8 represent the fractions eluted at pH 7.5, 7, 6.5, 6, 5.5, 4.0, respectively. At the end of the pH gradient, a solution of EDTA was applied (7 column volumes) to elute the remaining proteins (Lane 9). Lane 10 shows the molecular-weight standards (from the top): phosphorylase B (97,400), bovine serum albumin (66,200), ovalbumin (45,000), bovine carbonic anhydrase (31,000), soybean trypsin inhibitor (21,500), and lysozyme (14,400).

Table 1. Parameters Used in the Simulations

Parameter	Cytochrome	Lysozyme	Target
Molec. wt. (Da)*	12,700	14,300	15,000
Bulk diffus. (cm^2/s)**	1.08×10^{-6}	1.02×10^{-6}	1.01×10^{-6}
Intraparticle diffus. (cm^2/s)†	3.47×10^{-7}	3.16×10^{-7}	3.07×10^{-7}
Film mass-transfer coeff. (cm/s)††	1.08×10^{-3}	1.04×10^{-3}	1.02×10^{-3}
Particle dia. (cm)		0.0093	
Bed poros.‡		0.3333	
Particle poros.‡‡		0.92	
Col. height (cm)		2.55	
Superficial velo. (cm/s)		0.00848	
Axial dispers. coeff. (cm^2/s)§		4.21×10^{-4}	
Saturat. capac. (g/mL of particle phase)§§,‖		0.1	
Forward rate const.‖‖ (mL/g/s)		100	

*Value assumed for the target protein.
**Determined using the correlation of Young et al. (1980).
†Determined using the correlation of Boyer and Hsu (1992). The correlation is for Sepharose CL-6B, which is the base matrix for Chelating Sepharose Fast Flow, used in this study.
††Determined using the correlation of Ohashi et al. (1981).
‡Value supplied by Pharmacia Biotech (Piscataway, NJ).
‡‡Experimentally determined using the pulse elution with blank column (without copper).
§Determined using the correlation of Chung and Wen (1968).
§§Adjusted within 5% of the published value (see text for details).
‖Assumed the same for all three proteins due to approximately similar molecular weights (see text).
‖‖Set to simulate fast kinetics.

were obtained by fitting the experimental breakthrough curves with the model predictions (Figure 3). The B values are listed in Table 2.

Table 2 shows that, in general, the binding constants decrease with decreasing pH. The increase in the binding constant from pH 7.25 to pH 7.0 for lysozyme may reflect experimental error. The sharp drop in B from pH 7 to 6.5, followed by relatively constant values, between pH 6.5 and 6, may be due to the presence of multiple weak copper binding sites of lysozyme, which show noticeable binding at high pH

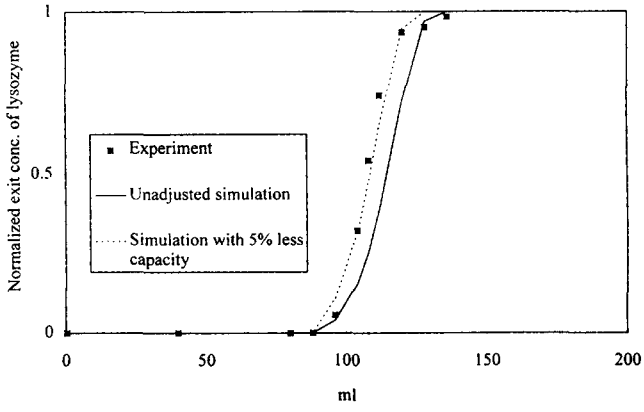

Figure 2. Model predictions vs. the experiment for the lysozyme breakthrough at pH 7.

Unadjusted simulation is with the literature values of B and q_m (Hutchens et al., 1988). The adjusted simulation is with 5% less saturation capacity than the literature value (Table 1).

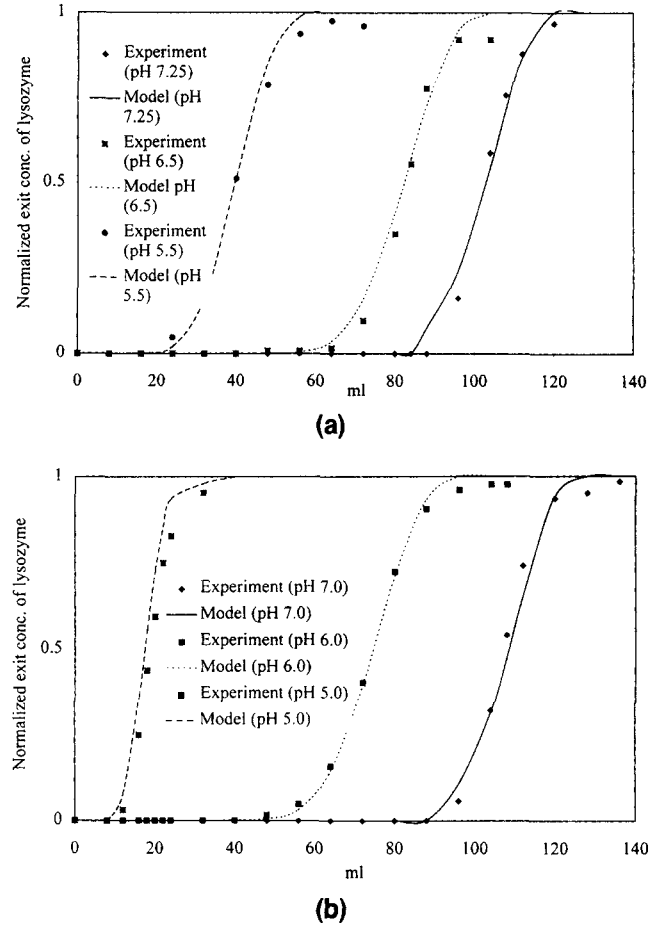

Figure 3. Model predictions vs. experimental breakthrough of lysozyme at different pH values.

The binding constant at each pH is determined based on the fit between the model and experiment [the pH values are grouped as shown in (a) and (b) in order to improve the clarity].

(e.g., pH 7.25 and 7.0), but lose their affinity as the pH is lowered to 6.5. Copper binding after this point could be predominantly due to the strong copper binding site of lysozyme, which is mainly responsible for its retention until low pH. Thus, the B values remain relatively constant between pH 6.5 and 6.0, and then start dropping rapidly as the elution pH (pH 5 for lysozyme), or the pKa of the strong binding site is approached.

Cytochrome. Due to the relatively high cost of cytochrome and large amounts typically needed for break-

Table 2. pH-Dependent Copper Binding Constants (mL/g)

pH	Cytochrome*	Lysozyme**
7.25	320	1380
7.0	72	1626
6.5	13.5	800
6.0	8	660
5.5	5	240
5.0	6	80

*Determined using zonal analysis (see text for details).
**Determined using breakthrough experiments (see text for details).

through experiments, breakthrough curves were not used for the estimation of its binding parameters with Cu-IDA. The high extinction coefficient of this protein and its low affinity for immobilized copper, allowed the use of zonal analysis for obtaining the values of the product Bq_m, at different pH values (Arnold et al., 1986). The values of B were then estimated by setting the saturation capacity of cytochrome to the same value as that of lysozyme. The assumption of equal saturation capacities of the two proteins is based on similar molecular weights (lysozyme: 14,300 Da and cytochrome: 12,700 Da). Table 2 shows the pH dependence of the binding constants. The sharp drop in binding constants of cytochrome between pH 7.25 and 7 is consistent with our prior observation that the value of B drops sharply in the vicinity of the elution pH of a protein (Patwardhan and Ataai, 1997).

Validation of model predictions

The model predictions, presented next, are performed using the values listed in Tables 1 and 2, without any adjustment. Figure 4 shows the comparison of the simulated breakthrough curves with experiments at different input concentrations. Note that the discrepancy between the model predictions and experiments increases in the later parts of the breakthrough and also, with increasing input concentrations. This is most likely the effect of assuming a constant intraparticle diffusivity, independent of adsorbed concentration. Intraparticle diffusivity often decreases with increasing adsorbed protein concentration, as the high amount of protein bound in the pores makes further diffusion relatively more difficult (Patwardhan and Ataai, 1997; Horstmann and Chase, 1989).

The breakthrough curves at different input concentrations, shown in Figure 4, were also used to obtain the binding constant of lysozyme at pH 6 by frontal analysis (Hutchens et al., 1988). This was done in order to confirm that the estimated binding constants in Table 2 are close to the actual ones and that the fits shown in Figure 3 are not due to a combination of different parameters. The value of binding constant, obtained from frontal analysis at pH 6, was about 600 mL/g, compared to 660 mL/g in Table 2.

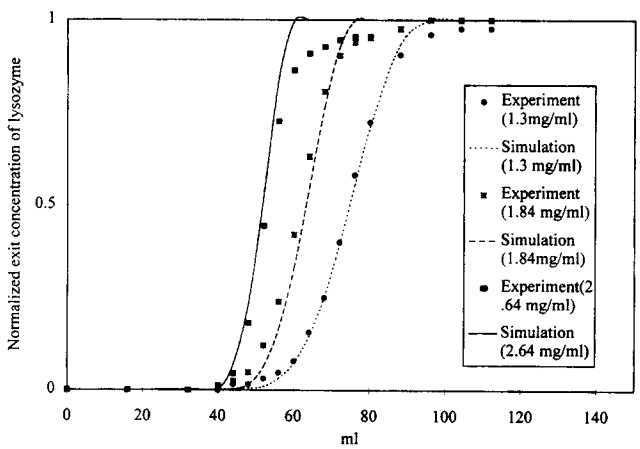

Figure 4. Model predictions vs. experimental breakthrough at different input concentrations at pH 6.

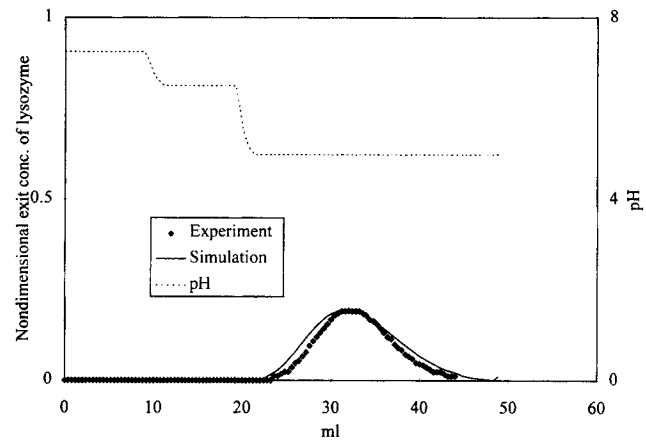

Figure 5. Simulation vs. experiment for the pulse elution of lysozyme, using the parameters in Tables 1 and 2.

A 3.5-mL pulse of lysozyme (1.54 mg/mL) is loaded on the column and eluted at a flow rate of 0.4 mL/min, with a step gradient in pH (output concentration is normalized with respect to the input concentration).

In Figures 5 and 6 model predictions are compared with the pulse elution experiment for lysozyme and cytochrome, respectively. Satisfactory fits are obtained for the elution of both proteins without adjusting the parameters. Figure 7 shows the model predictions for the pulse elution experiment performed using a mixture of lysozyme and cytochrome. Small discrepancies between the simulations and experiments may reflect experimental errors or the errors in the estimates of mass-transfer coefficients and equilibrium parameters. In summary, Figures 4 to 7 show that the model accurately predicts the adsorption and elution of single as well as multiple proteins from the Cu-IDA column. Next, the results of the simulations using the validated model are discussed.

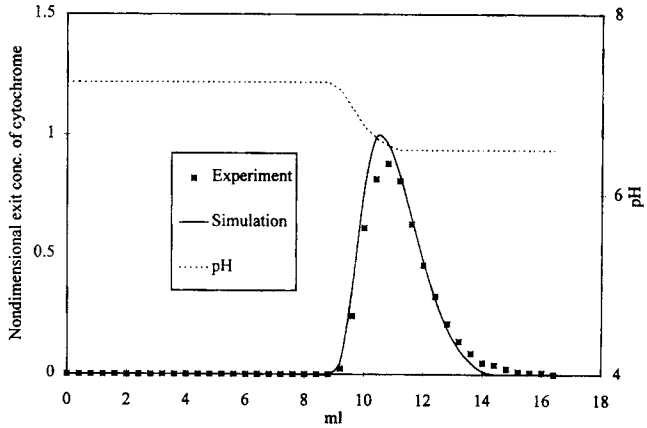

Figure 6. Simulation vs. experiment for the pulse elution of cytochrome, using the parameters in Tables 1 and 2.

A 2.6-mL pulse of cytochrome (2.76 mg/mL) is loaded on the column and eluted at a flow rate of 0.4 mL/min, with a step gradient in pH (output concentration is normalized with respect to the input concentration).

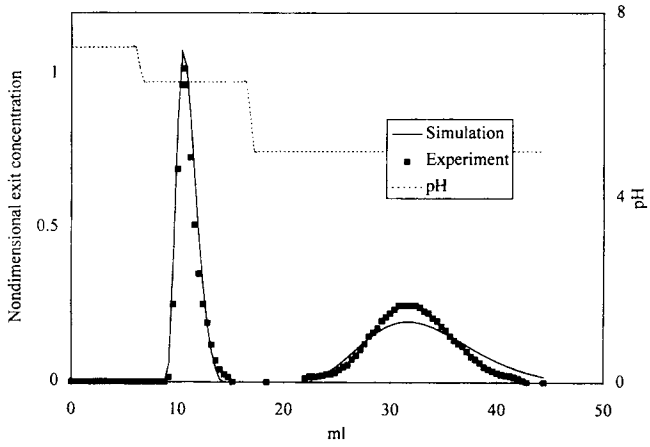

Figure 7. Simulation vs. experiment for the pulse elution of a mixture of cytochrome and lysozyme, using the parameters in Tables 1 and 2.

A 3.5-mL pulse (2.97-mg/mL cytochrome and 1.6-mg/mL lysozyme) is loaded on the column and eluted at a flow rate of 0.4 mL/min, with a step gradient in pH (output concentration is normalized with respect to the input concentration of each protein).

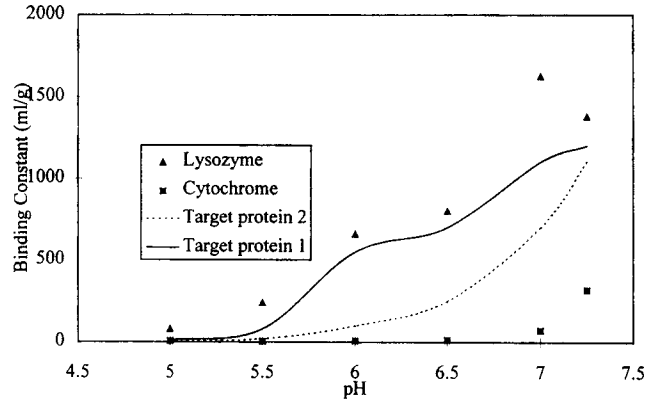

Figure 8. pH dependence of the binding constants of target proteins, tuna heart cytochrome c, and chicken egg white lysozyme with immobilized copper.

The B values for cytochrome and lyszoyme are from Table 2. The values for target proteins are assumed as discussed in the text.

Simulation results

Typically, in IMAC experiments, protein mixtures are loaded at high pH (Le Grice and Leitch, 1990; Crowe et al., 1994). The goal of the simulations was to assess the effect of loading pH on the column capacity and purification of the target protein from the *E. coli* cell extract.

As noted, the *E. coli* cell extract was represented by two model proteins, cytochrome and lysozyme. The loading mixture in all the simulations contained 80% cytochrome, 10% lysozyme, and 10% target protein. The ratio of cytochrome and lysozyme (8:1), is approximately similar to the proportion of the weak and strong copper binding proteins of *E. coli* (Figure 1).

Two target proteins were considered. Their binding constants with Cu-IDA were selected such that they will elute at a pH between the elution pH of cytochrome and lysozyme (Figure 8). The pH dependence of the binding constants of target protein 1 (Figure 8) was chosen to be similar to that of lysozyme but with B values lower than those of lysozyme at each pH. The B values of target protein 2 were selected to fall between those of target protein 1 and cytochrome. First, we discuss the results of the simulations for target protein 1.

The simulations were performed for the loading of a mixture of three proteins (cytochrome, lysozyme, and the target protein) at various pH values (pH 7.25, 6.5, 6.0 and 5.5). The amount of target protein and contaminants (i.e., lysozyme + cytochrome) bound in the column were calculated, in each case, after the exit concentration of the target protein reached 20% of its input value. This was done in order to parallel the general practice of terminating the loading step before the outlet concentration of the target protein reaches a high value, thus avoiding significant losses of the target protein (Arnold, 1985).

Figure 9 shows the effect of loading pH on the amount of cytochrome and lysozyme adsorbed on the column. As expected, loading at a lower pH (e.g., pH 6.5 and lower) as opposed to pH 7.25, resulted in a lower amount of total bound contaminants (i.e., lysozyme + cytochrome). This decrease is primarily due to the corresponding decrease in the adsorbed amount of cytochrome, between pH 7.25 and 6.5. Figure 9 also shows the effect of the loading pH on the adsorbed concentration of the target protein. The adsorbed amount of target protein was also higher at pH 6.5 and 6 than at pH 7.25. This trend is in contrast to the values of binding constants for the target protein plotted in Figure 8 (i.e., B values of 700 and 550 mL/g at pH 6.5 and 6, respectively, compared to 1200 mL/g at pH 7.25). Lower copper affinity of the target protein at low pH is expected to result in a decreased amount of adsorbed target protein, leading to a loss in capacity. The trend shown in Figure 9, however, arises due to the elimination of a large amount of contaminants (lysozyme + cytochrome) from the column, hence, the availability of a

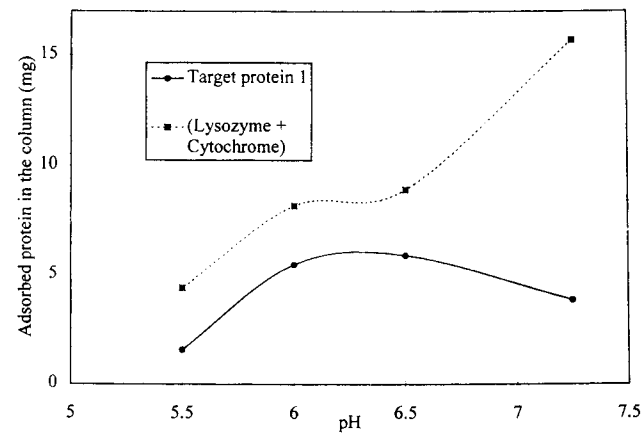

Figure 9. Simulated effect of the loading pH on the amount of lysozyme, cytochrome (representing impurities) and target protein 1 bound on the column.

The values are calculated when the exit concentration of target protein 1 reaches 20% of its input value.

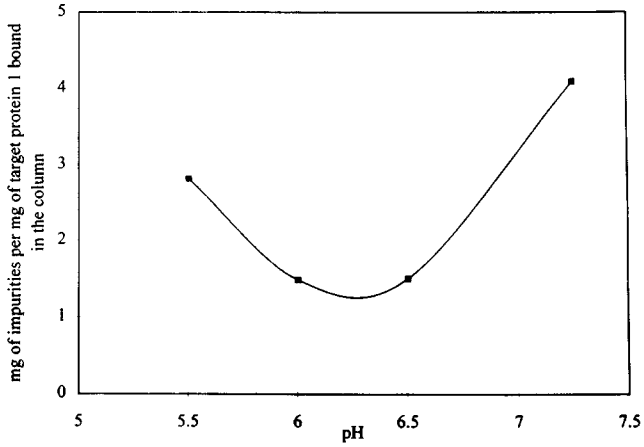

Figure 10. Effect of loading pH on grams of impurity (lysozyme+cytochrome) per gram of target protein 1 bound in the column.

Ratios are calculated when the exit concentration of target protein 1 reaches 20% of its input value.

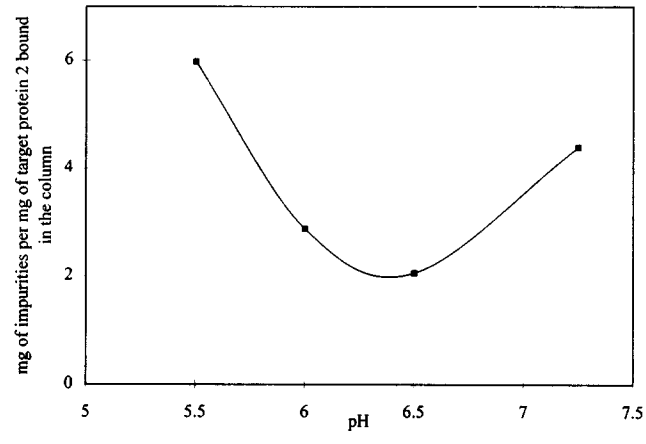

Figure 11. Effect of loading pH on grams of impurity (lysozyme+cytochrome) per gram of target protein 2 bound in the column.

Ratios are calculated when the exit concentration of target protein 2 reaches 20% of its input value.

larger number of copper sites for the adsorption of target protein.

Figure 10 shows the ratio of the adsorbed contaminants (cytochrome + lysozyme) to the target protein bound in the column at each loading pH. Comparison of Figures 9 and 10 clearly demonstrates the benefits of loading the protein mixture at an intermediate pH value (between pH 6.5 and 6.0), as opposed to loading at a higher pH. First, note that loading at pH between 6.5 and 6.0 led to a higher amount of target protein adsorbed on the column, compared to loading at pH 7.25 (i.e., 5.9 mg vs. 3.8 mg). Moreover, Figure 10 demonstrates that the ratio of the bound impurities (i.e., lysozyme + cytochrome) to the bound target protein is substantially lower at pH 6.5 (1.4) than that at pH 7.25 (4.3). Thus, in summary, loading at an optimum pH of 6.5 to 6.0, increases the amount of bound target protein and decreases the bound impurities.

In order to confirm that the preceding advantages were not specific to the particular kind of pH dependence that was assigned to the binding constants of the target protein, simulations were also performed for another target protein (i.e., target protein 2 in Figure 8) with a different pH dependence. The values of B were chosen such that this protein will also elute at a pH between the elution pH of the two contaminants but, in general, will have a lower copper affinity than the previous target protein (Figure 8). The simulation results, presented in Figure 11, demonstrate that even for a target protein that has a relatively weaker affinity toward Cu-IDA, the ratio of the bound target protein to contaminants (i.e., lysozyme + cytochrome) is higher when the protein mixture is loaded at pH 6.5 and 6.0, than at pH 7.25.

Summary

In summary, this investigation reports detailed mathematical modeling of the influence of loading pH on the purity and binding capacity of target proteins during their purification from the *E. coli* cell extract using a Cu(II)-IDA column. The elution behavior of the *E. coli* cell extract was characterized by two peaks separated by a contaminant-free region. Thus, the cell extract was simulated using a mixture of two model proteins. The binding and transport parameters of these proteins were evaluated using experiments and literature correlations. The parameters were incorporated into a detailed model of multicomponent chromatography. Target proteins eluting in the contaminant-free region of the *E. coli* cell extract were also included in the formulation. The predictions of the model were validated experimentally and simulations were performed to assess the effect of loading pH on the binding capacity and purity of the target proteins. The results demonstrated that loading the protein mixture at an intermediate pH of 6.5 to 6, as opposed to a high pH of 7.25, not only resulted in decreased binding of the impurities but also led to higher binding capacities of the target protein.

Acknowledgment

This work was supported by a grant from the Whitaker Foundation to one of the authors (M. M. A.).

Notation

B_i = binding constant of protein metal interaction (mL/g)
C_{b_i} = bulk protein concentration, g/mL
C_{f_i} = feed concentration of proteins, g/mL
C_{p_i} = pore concentration of protein, g/mL
D_{p_i} = intraparticle diffusivity of the protein, cm^2/s
D_{b_i} = axial dispersion coefficient, cm^2/s
$D_{ab,i}$ = bulk diffusivity, cm^2/s
H = height of the column, cm
k_i = film mass-transfer coefficient, cm/s
k_{pri} = partition coefficient of the protein molecules
k_a = forward (adsorption) rate constant, mL/(g·s)
k_d = reverse (desorption) rate constant, s
Mw_i = molecular weight, Da
n = total number of protein species
q_i = bound protein concentration in the solid phase (g/mL of the solid phase)
R = radius of the pellet, cm
r = radial coordinate, cm
v = superficial velocity, cm/s
x = axial coordinate, cm
ϵ_{p_i} = particle porosity for each protein
ϵ_b = bed porosity of the column
q_m = saturation capacity of the column for the protein (g/mL of solid phase)

Literature Cited

Anderson, L., E. Sulkowski, and J. Porath, "Immobilized Metal Ion Affinity Chromatography of Serum Proteins," *Bioseparations*, **2**, 15 (1991).

Arnold, F. H., S. A. Schofield, and H. W. Blanch, "Analytical Affinity Chromatography: I. Local Equilibrium Theory and the Measurement of Association and Inhibition Constants," *J. Chromatog.*, **355**, 1 (1986).

Arnold, F. H., H. W. Blanch, and C. R. Wilke, "Analysis of Affinity Separations: I. Predicting the Performance of Affinity Adsorbers," *Chem. Eng. J.*, **30**, B9 (1985).

Beitle, R. R., and M. M. Ataai, "One Step Purification of a Model Periplasmic Protein from Inclusion Bodies by its Fusion to an Effective Metal Binding Peptide," *Biotechnol. Prog.*, **9**, 64 (1993).

Beitle, R. R., and M. M. Ataai, "Immobilized Metal Affinity Chromatography and Related Techniques," *AIChE Symp. Ser.: New Developments in Bioseparation*, **88**, 34 (1992).

Binous, H., and B. J. McCoy, "Chromatographic Reactions of Three Components: Applications to Separations," *Chem. Eng. Sci.*, **47**, 4333 (1992).

Boyer, P. M., and J. T. Hsu, "Experimental Studies of Restricted Protein Diffusion in Agarose Matrix," *AIChE J.*, **38**, 259 (1992).

Chung, S. F., and C. Y. Wen, "Longitudinal Dispersion of Liquid Flowing Through Fixed and Fluidized Beds," *AIChE J.*, **14**, 857 (1968).

Crowe, J., H. Dobeli, R. Gentz, E. Hochuli, D. Stuber, and K. Henco, "6xHis-Ni-NTA Chromatography as a Superior Technique in Recombinant Protein Expression/Purification," *Methods Mol. Biol.*, **31**, 371 (1994).

Dunn, M. B., "The Study of Ligand-Protein Interactions Utilizing Affinity Chromatography," *Appl. Biochem. Biotechnol.*, **9**, 261 (1984).

Gallant, S., A. Kundu, and S. M. Cramer, "Optimization of Step Gradient Separations: Consideration of Nonlinear Adsorption," *Biotechnol. Bioeng.*, **47**, 355 (1995).

Golshan-Shirazi, S., and G. Guiochon, "Theoretical Study of System Peaks and Elution Profiles of High Concentration Bands of Binary Mixtures Eluted by a Binary Eluent Containing a Strongly Retained Additive," *Anal. Chem.*, **61**, 2373 (1989).

Goud, N., A. Patwardhan, M. Ataai, and R. Koepsel, "Selection of Specific Peptide Ligands for Immobilized Metals Using a Phage Displayed Library: Application to Protein Separation Using IMAC," *Int. J. Biochromatog.*, (1996).

Gu, T., G. Tsai, and G. T. Tsao, "Multicomponent Adsorption and Chromatography with Uneven Saturation Capacities," *AIChE J.*, **37**, 1333 (1991).

Gu, T., Y. Truei, G. Tsai, and G. T. Tsao, "Modeling of Gradient Elution in Multicomponent Nonlinear Chromatography," *Chem. Eng. Sci.*, **47**, 253 (1992).

Hemdan, E. S., Y. Zhao, E. Sulkowski, and J. Porath, "Surface Topography of Histidine Residues: A Facile Probe by Immobilized Metal Ion Affinity Chromatography," *Proc. Nat. Acad. Sci. U.S.*, **86**, 1811 (1989).

Hochuli, E., W. Bannwarth, H. Dobeli, R. Gentz, and D. Stuber, "Genetic Approach to Facilitate Purification of Recombinant Proteins with a Novel Metal Chelate Absorbent," *Bio/Technol.*, **6**, 1321 (1988).

Horstmann, B. J., and H. A. Chase, "Modeling the Affinity Adsorption of the Immunoglobulin G to Protein A Immobilized to Agarose Matrix," *Chem. Eng. Res. Dev.*, **67**, 243 (1989).

Hutchens, T., T. Yip, and J. Porath, "Protein Interaction with Immobilized Ligands: Quantitative Analysis of the Equilibrium Partition Data and Comparison with Analytical Chromatographic Approaches Using Immobilized Metal Affinity Adsorbents," *Anal. Biochem.*, **170**, 168 (1988).

IMSL, *IMSL User's Manual: FORTRAN Subroutines for Mathematical Applications*, Version 2.0, IMSL, Houston, p. 755 (1991).

Le Grice, S. F. J., and F. G. Leitch, "Rapid Purification of Homodimer and Heterodimer HIV-1 Reverse Transcriptase by Metal Chelate Affinity Chromatography," *Eur. J. Biochem.*, **187**, 307 (1990).

Ohashi, H., T. Sugawara, K. Kicuchi, and H. Konno, "Correlation of Liquid-side Mass Transfer Coefficient for Single Particles and Fixed Beds," *J. Chem. Eng. Jpn.*, **14**, 433 (1981).

Patwardhan, A. V., and M. Ataai, "One Step Purification of Human Interleukin 1β from the Cellular Proteins of *E. coli* Using the Immobilized Metal Affinity Chromatography," *Int. J. Biochromatog.*, **2**, 119 (1996).

Patwardhan, A. V., and M. M. Ataai, "Site Accessibility and the pH Dependence of the Saturation Capacity of a Highly Cross-linked Matrix: Immobilized Metal Affinity Chromatography of BSA on Chelating Superose," *J. Chromat. A*, (1997).

Patwardhan, A., N. Goud, R. Koepsel, and M. Ataai, "Selection of Optimum Affinity Tags from a Phage Displayed Peptide Library: Application to Immobilized Copper Affinity Chromatography," (1997a).

Patwardhan, A., N. Goud, R. Koepsel, and M. Ataai, "Phage-Displayed Libraries for the Selection of Optimal Affinity Tails for Ni-NTA Purification of Recombinant Proteins," (1997b).

Porath, J., J. Carlsson, I. Olsson, and G. Belfrage, "Metal Chelate Affinity Chromatography, A New Approach to Protein Purification," *Nature*, **258**, 598 (1975).

Porath, J., and B. Olin, "Immobilized Metal Ion Affinity Adsorption and Immobilized Metal Ion Affinity Chromatography of Biomaterials. Serum Protein Affinities for Gel Immobilized Iron and Nickel Ions," *Biochemistry*, **22**, 1621 (1983).

Velayudhan, A., and M. R. Ladisch, "Effect of Modular Sorption on Gradient Shape in Ion Exchange Chromatography," *Ind. Eng. Chem. Res.*, **34**, 2805 (1995).

Vosters, A. F., D. B. Evans, W. G. Tarpley, and S. K. Sharma, "On the Engineering of rDNA Proteins for Purification by Immobilized Metal Affinity Chromatography: Applications to Alternative Histidine Containing Chimeric Proteins from Recombinant *Escherichia coli*," Protein Expr. Purif., **3**, 18 (1992).

Whitley, R. D., X. Zhang, and N. H. L. Wang, "Protein Denaturation in Nonlinear Isocratic and Gradient Elution Chromatography," *AIChE J.*, **40**, 1067 (1994).

Young, M. E., P. A. Caproad, and R. L. Bell, "Estimation of the Diffusion Coefficients of the Proteins," *Biotechnol. Bioeng.*, **22**, 947 (1980).

Manuscript received Feb. 5, 1997, and revision received June 12, 1997.